Symmetry Aspects in the Use of Multilayered Substrates for SAW Devices

Natalya F. Naumenko, *Member, IEEE*

***Abstract*— Multilayered structures extensively studied as a novel type of substrates for surface acoustic wave (SAW) devices are characterized by an asymmetry of wave propagation: acoustic wave characteristics generally change with inversion of propagation direction or interchange of top/bottom surfaces in one of the layers, though separately each material is symmetric for such inversions. In this article, the matrix formalism known as an effective tool for theoretical and numerical investigation of acoustic wave propagation in multilayered structures is applied to explain the existence of asymmetry and analyze its relation to the symmetry and orientations of combined materials. This phenomenon is illustrated by the examples of layered structures combining $LiTaO_3$ (LT) plate with quartz or Si, previously reported as potential substrates for SAW devices with improved performance. Asymmetry arises from anisotropy of combined materials and occurs even when one of these materials is non-piezoelectric. It was estimated numerically as a variation of SAW resonator characteristics with substrate or plate inversion and was analyzed as a function of plate or substrate orientation. In particular, it was shown that "polarity inverted" structure enabling alternative resonator performance for the same material layers can be obtained either by an interchange of top/bottom surfaces of a piezoelectric plate or by inversion of propagation direction in a substrate. Asymmetry decreases with the introduction of an isotropic layer at the plate-substrate interface.**

***Index Terms*— Anisotropy, multilayered structure, reciprocity, surface acoustic wave (SAW) propagation, SAW resonator.**

I. Introduction

LAYERED structures combining material layers with different properties are a novel and most promising type of substrates for new generations of surface acoustic wave (SAW) devices [1]–[7]. Application of layered substrates breaks the limitations of regular single crystal substrates and facilitates the development of SAW devices with higher operating frequencies, lower insertion losses, wider bandwidths, better thermal stability, and improved quality (Q) factors of SAW resonators. However, the application of layered substrates is followed by some new features, which characterize acoustic wave behavior and must be taken into account in the fabrication of layered substrates and their further use. In particular, SAW velocity, electromechanical coupling, and other wave characteristics generally change with inversion of propagation direction in one of the combined materials or interchange of top/bottom surfaces of a layer [8], [9], though separately each material is "symmetric" for such inversions, as follows from the general principle of reciprocity valid for acoustic waves [10].

The aforementioned asymmetry [11] of wave propagation in layered structures manifests itself, for example, by a variation of the performance of SAW resonators built on initial and inverted structures. This asymmetry was observed experimentally in resonators arranged on thin $LiTaO_3$ (LT) plates bonded to quartz [8] as different behaviors of SAW resonators based on the structures with "positive" or "negative" LT plane bonded to a quartz substrate. The variation of wave characteristics in a layered structure with interchange of top and bottom surfaces of a thin plate requires careful control of orientations of combined crystals before their bonding. However, it is also a simple method of modifying device performance without changing crystal orientations.

Generally, acoustic wave characteristics in layered structures also change with the inversion of propagation direction in one of the combined materials. The effect of such inversion on resonator performance was previously investigated for thin $LiNbO_3$ (LN) plates bonded to quartz substrates [9], [11]. The simulations revealed that the electromechanical coupling coefficient (k^2) changes by 25% of its value with inversion of propagation direction in some structures, while the variation of temperature coefficients of frequency (TCF) can achieve 7 ppm/°C. In the analyzed structures, 180° rotation of a substrate around the vertical axis was equivalent to an interchange of top and bottom surfaces of a plate and could be used as a less laborious method of fabricating layered structures with alternative acoustic wave characteristics.

In this article, the described phenomenon of asymmetry of wave propagation in layered structures is studied theoretically (Section II) and illustrated by a few examples combining piezoelectric LT plate with a non-piezoelectric (silicon) or piezoelectric (quartz) substrate (Section III). The asymmetry of wave propagation was investigated as a function of plate and substrate orientations to understand its relation to the symmetry and anisotropy of combined materials, as well as

Manuscript received March 24, 2022; accepted April 20, 2022. Date of publication April 22, 2022; date of current version May 26, 2022. This work was supported in part by the Russian Science Foundation under Grant 20-12-00348.

The author is with the Acoustooptical Research Center, National University of Science and Technology MISIS, 119049 Moscow, Russia, and also with the Research Department, Moscow Technical University of Communications and Informatics, 111024 Moscow, Russia (e-mail: nnaumenko@ieee.org).

Digital Object Identifier 10.1109/TUFFC.2022.3169808

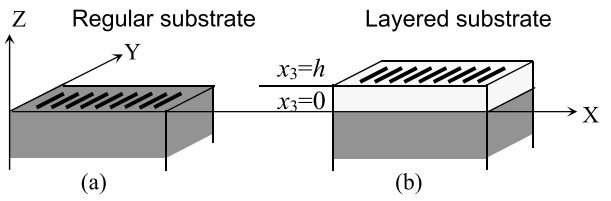

Fig. 1. (a) Schematic of regular substrate and (b) layered substrate for SAW devices with coordinate axes *X*, *Y*, and *Z*.

to polarization and piezoelectric coupling of acoustic modes propagating in the analyzed structures.

II. Matrix Formalism for SAW Propagating in Layered Structures

Acoustic waves propagating in a half-infinite piezoelectric medium must satisfy the field equations

$$\rho \frac{\partial^2 u_j}{\partial t^2} = c_{ijkl} \frac{\partial^2 u_l}{\partial x_i \partial x_k} + e_{kij} \frac{\partial^2 \varphi}{\partial x_i \partial x_k} \tag{1}$$

$$e_{kij} \frac{\partial^2 u_i}{\partial x_k \partial x_j} - \varepsilon_{ik} \frac{\partial^2 \varphi}{\partial x_i \partial x_k} = 0 \tag{2}$$

where u_i are components of mechanical displacement vector, φ is electrostatic potential, c_{ijkl}, e_{kij}, and ε_{ik} are the tensors of elastic stiffness, piezoelectric constants, and dielectric permittivity, respectively, and ρ is the mass density. The surface wave solutions are generally four-partial

$$u_i = \sum_{n=1}^{4} C_n \cdot u_i^n \cdot \exp\left(jk\alpha^n x_3\right) \cdot \exp[jk(x_1 - Vt)] \tag{3}$$

$$\varphi = \sum_{n=1}^{4} C_n \cdot \varphi^n \cdot \exp\left(jk\alpha^n x_3\right) \cdot \exp[jk(x_1 - Vt)] \tag{4}$$

and built by the modes with attenuation coefficients α^n satisfying the requirement of amplitude attenuation with the depth. The subscripts "1," "2," and "3" in (1)–(4) are referred, respectively, to the coordinates along *X*-, *Y*-, and *Z*-axes of the specified substrate orientation, as shown in Fig. 1(a). The amplitude coefficients in (3) and (4) can be determined from the boundary conditions on the substrate surface ($x_3 = 0$).

The unknown characteristics of partial modes u_i^n, φ^n, and α^n are calculated by solving the eigenmode problem [12], [13]

$$\hat{A}\boldsymbol{\tau} = \alpha\boldsymbol{\tau} \tag{5}$$

where $\hat{A}$ is the fundamental acoustic tensor dependent on material constants rotated according to the specified Euler angles (φ, θ, ψ) of a substrate, and the 8-D eigenvectors $\boldsymbol{\tau} = \left(\boldsymbol{L}, j\omega\boldsymbol{U}\right)$ are composed by the generalized stress $\boldsymbol{L}$ and displacement $\boldsymbol{U}$ vectors

$$\boldsymbol{L} = (T_{31}, T_{32}, T_{33}, D_3) \tag{6}$$

$$\boldsymbol{U} = (u_1, u_2, u_3, \varphi). \tag{7}$$

The eigenvectors $\boldsymbol{\tau}$ are usually combined into the 8 × 8 state matrix $\hat{\Psi}$, which characterizes the analyzed material

$$\hat{\Psi} = \left\{ \hat{\Psi}^{(-)}, \hat{\Psi}^{(+)} \right\} = \begin{Bmatrix} \hat{L}^{(-)} & \hat{L}^{(+)} \\ \hat{U}^{(-)} & \hat{U}^{(+)} \end{Bmatrix} \tag{8}$$

where $\hat{L}^{(-)}$ and $\hat{U}^{(-)}$ are 4 × 4 matrices of stresses and displacements associated with the four "downward" partial modes. For pure SAW solutions, the amplitudes of these modes attenuate with the depth. Leaky waves (LSAWs) include one or two quasi-bulk modes, which leak slowly into the depth. These four modes build physically acceptable SAW or LSAW solutions. The matrices $\hat{L}^{(+)}$ and $\hat{U}^{(+)}$ refer to the remaining "upward" modes with amplitudes growing into the depth and unphysical for the analyzed substrate geometry. After inversion of propagation direction, the physically acceptable SAW solutions must be built by $\hat{L}^{(+)}$ and $\hat{U}^{(+)}$ instead of $\hat{L}^{(-)}$ and $\hat{U}^{(-)}$.

The eigenmodes of the fundamental acoustic tensor satisfy the orthogonality relation [12], which can be transformed into the following equation [14]:

$$\hat{L}^{(-)} \cdot \left[\hat{U}^{(-)}\right]^{-1} + \left[\hat{U}^{(+)T}\right]^{-1} \cdot \hat{L}^{(+)T} = 0 \tag{9}$$

or

$$\hat{Z}^{(-)} + \hat{Z}^{(+)T} = 0 \tag{10}$$

where

$$\hat{Z}^{(-)} = \hat{L}^{(-)} \cdot \left[\hat{U}^{(-)}\right]^{-1} \tag{11a}$$

$$\hat{Z}^{(+)} = \hat{L}^{(+)} \cdot \left[\hat{U}^{(+)}\right]^{-1} \tag{11b}$$

are the 4 × 4 impedance matrices referred to the downward and upward modes, respectively. Both matrices are determined by the state matrix (8) of a half-infinite medium. They characterize the ratio between the stresses and displacements at any plane parallel to the boundary.

In a multilayered structure, the use of impedance matrices enables the easy formulation of boundary conditions at the interfaces, due to their continuous transformation across the boundaries of the layers. For example, at the interface between *n*th and $(n-1)$th layers

$$\det\left(\hat{Z}_n - \hat{Z}_{n-1}\right) = 0. \tag{12}$$

The relationship between the upward and downward modes described by (10) means the reciprocity for acoustic waves propagating in a half-infinite medium: the wave propagation always occurs in a symmetrical fashion, with the same velocity in initial and reversal directions. Though the reciprocity theorem was first proved for pure elastic surface waves [10], it is a basic property of SAWs or leaky SAWs propagating in a piezoelectric crystal.

In a substrate covered by one or a few overlays [see Fig. 1(b)], the impedance matrix depends on the coordinate x_3 along *Z*-axis and can be calculated as a ratio of stress and displacement vectors

$$\hat{Z}(x_3) = \boldsymbol{L}(x_3) \cdot [\boldsymbol{U}(x_3)]^{-\mathbf{1}}. \tag{13}$$

For example, on top of a layered structure ($x_3 = h$) with a thin film of thickness h arranged over a half-infinite substrate, as shown in Fig. 1(b), the impedance matrix is

calculated as [15]

$$\hat{Z}_{x3=h} = \left\{\hat{Z}^{(-)}\cdot\hat{\Lambda}^{(-)}\cdot\left[\hat{Z}^{(-)}-\hat{Z}^{(+)}\right]^{-1}\cdot\left[\hat{Z}_S-\hat{Z}^{(+)}\right] - \hat{Z}^{(+)}\cdot\hat{\Lambda}^{(+)}\cdot\left[\hat{Z}^{(-)}-\hat{Z}^{(+)}\right]^{-1}\cdot\left[\hat{Z}_S-\hat{Z}^{(-)}\right]\right\} \cdot\left\{\hat{\Lambda}^{(-)}\cdot\left[\hat{Z}^{(-)}-\hat{Z}^{(+)}\right]^{-1}\cdot\left[\hat{Z}_S-\hat{Z}^{(+)}\right] - \hat{\Lambda}^{(+)}\cdot\left[\hat{Z}^{(-)}-\hat{Z}^{(+)}\right]^{-1}\cdot\left[\hat{Z}_S-\hat{Z}^{(-)}\right]\right\}^{-1} \quad (14)$$

where $\hat{Z}^{(-)}$ and $\hat{Z}^{(+)}$ are the impedance matrices of the downward and upward modes in the layer, $\hat{Z}_S$ is the impedance matrix of the downward modes in a substrate, and $\hat{\Lambda}^{(-)}$ and $\hat{\Lambda}^{(+)}$ are the diagonal matrices of propagators with components

$$\Lambda_{ii}^{(-)} = \exp\left(2\pi\cdot\alpha_i^{(-)}\cdot h/\lambda\right) \quad (15a)$$

$$\Lambda_{ii}^{(+)} = \exp\left(2\pi\cdot\alpha_i^{(+)}\cdot h/\lambda\right) \quad (15b)$$

responsible for the transformation of displacements between the bottom ($x_3 = 0$) and top ($x_3 = h$) surfaces of the layer.

If the layer thickness tends to zero, (14) yields $\hat{Z} = \hat{Z}_S$. For layer and substrate made of the same material $\hat{Z} = \hat{Z}^{(-)} = \hat{Z}_S$. In a more general case, acoustic fields in the layer are built by the upward and downward layer modes and by the downward substrate modes. The contributions of the upward layer modes and substrate modes are determined by the reflection and transmission coefficients at the substrate-layer interface. These contributions decrease and finally vanish with growing layer thickness. The equations, which allow rigorous simulation of acoustic fields in each layer of a multilayered structure, were previously derived [6], [16] and used for a thorough numerical investigation of acoustic fields in different layered structures [17]–[20].

The asymmetry of acoustic wave propagation in a layered structure can be deduced from (14). With inversion of propagation direction in both materials of a layered structure simultaneously, the matrix $\hat{Z}$ changes to its transpose and the velocities of acoustic waves do not change with such inversion. Hence, the reciprocity is valid for acoustic waves in a fixed layered structure. If only substrate or only plate is rotated by 180° around the Z-axis, it can be described by the following transformation of the axes, which characterize the substrate orientation: $X \to -X$, $Y \to -Y$, or by rotation matrix:

$$\hat{a}_Z = \begin{pmatrix} -1 & 0 & 0 & 0 \\ 0 & -1 & 0 & 0 \\ 0 & 0 & 1 & 0 \\ 0 & 0 & 0 & 1 \end{pmatrix}. \quad (16)$$

Then, the impedance matrix of the inverted substrate can be derived

$$\hat{Z}_S^{\text{inv}} = \hat{a}_Z\hat{Z}_S\hat{a}_Z. \quad (17)$$

Some components of the impedance matrix $\hat{Z}_S$ change the sign with inversion of the propagation direction, while other components do not change. The components of the matrix $\hat{Z}_S$ changing the sign with 180° rotation of the substrate around the Z-axis are Z_{13}, Z_{23}, Z_{14}, Z_{24}, Z_{31}, Z_{32}, Z_{41}, and Z_{42}. Then, the initial $\hat{Z}_S$ and inverted $\hat{Z}_S^{\text{inv}}$ matrices include symmetric

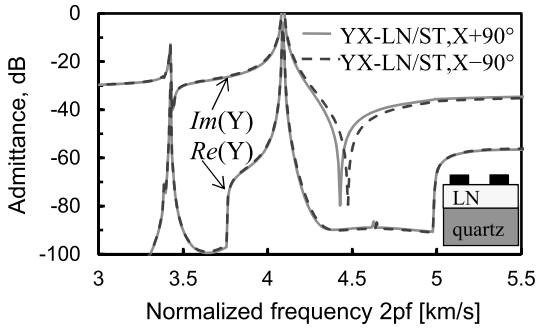

Fig. 2. Example of admittance functions obtained for resonators using *YX*-LN plate with Euler angles (0°, −90°, 0°) bonded to ST-quartz substrate with Euler angles (0°, −47.25°, 90°) or (0°, −47.25°, −90°).

$\hat{Z}_S^{\text{sym}}$ and anti-symmetric $\hat{Z}_S^{\text{asym}}$ contributions regarding the analyzed transformation of the substrate orientation

$$\hat{Z}_S = \hat{Z}_S^{\text{sym}} + \hat{Z}_S^{\text{asym}} \quad (18a)$$

$$\hat{Z}_S^{\text{inv}} = \hat{Z}_S^{\text{sym}} - \hat{Z}_S^{\text{asym}}. \quad (18b)$$

If either $\hat{Z}_S^{\text{sym}}$ or $\hat{Z}_S^{\text{antisym}}$ vanishes in the analyzed substrate orientation, then the matrix Z defined by (14) does not change with inversion of propagation direction in a substrate or transforms to its transpose, and all acoustic waves propagate with the same velocities in initial and inverted structures. If both contributions are nonzero, then in the terms $\left[\hat{Z}_S-\hat{Z}^{(+)}\right]$ and $\left[\hat{Z}_S-\hat{Z}^{(-)}\right]$ responsible for interactions between the substrate and layer modes, $\hat{Z}_S^{\text{asym}}$ is added to $\hat{Z}_S^{\text{sym}}$ with opposite signs. This difference gives rise to an asymmetry between the wave propagation velocities in the initial and inverted structures. The described asymmetry depends on the polarization of the analyzed acoustic wave. It does not occur if the displacement and stress components responsible for asymmetry are decoupled with the analyzed type of acoustic wave.

The aforementioned asymmetry effect cannot be explained only by the inversion of electric fields (electric polarity inversion [8]) in one of the combined materials. Even in a structure with a piezoelectric layer on a non-piezoelectric but anisotropic substrate, the characteristics of acoustic waves generally change with 180° rotation of a substrate. The same effect can be achieved if the substrate orientation is fixed and the layer is rotated. In this case, asymmetry is caused by the anti-symmetric terms added to $\hat{Z}^{(+)}$ and $\hat{Z}^{(-)}$ matrices. Moreover, the rotation of a substrate or layer around Z-axis can be replaced by two rotations, around X-axis (matrix $\hat{a}_X$) and around Y-axis (matrix $\hat{a}_Y$), or $\hat{a}_Z = \hat{a}_X\cdot\hat{a}_Y$.

Let us consider an example of a layered structure, which includes quartz substrate defined by the Euler angles (0°, μ, 90°) and LN plate with the angles (0°, θ, 0°). If the substrate is rotated by 180° around Z-axis, its Euler angles switch to (0°, μ, −90°), and acoustic wave velocities change. The influence of such rotation on the admittance of the SAW resonator can be observed in Fig. 2. The same acoustic wave characteristics occur if the LN plate is rotated around the X and Y axes instead of the Z-axis. Rotation around X-axis transforms the Euler angles of LN plate into (0°, 180° + θ, 0°), while rotation around Y-axis transforms them into (180°, −θ, 0°). Further rotation around Y-axis (in the first case) or around X-axis

TABLE I
TWO TYPES OF LN/QUARTZ STRUCTURES FOR SH-SAW RESONATORS, OBTAINED BY SUBSTRATE AND PLATE ROTATIONS

Quarts orientation	Initial (0,θ,0)	X-rotated (0,θ+180,0)	Y-rotated (180,−θ,0)	Z-rotated (0,θ,180)
Initial (0, μ, 90)	+	−	−	−
X-rotated (0, 180+μ, 90)	+	−	−	−
Y-rotated (180, −μ,90)	−	+	+	+
Z-rotated (0, μ,−90)	−	+	+	+

(in the second case) does not change the behavior of acoustic waves in the LN/quartz structure, due to the symmetry of LN crystal. Hence, the inversion of the LN/quartz structure can be achieved by one of the following rotations:

1) 180° rotation of quartz substrate around Z-axis;
2) 180° rotation of LN plate around Z-axis;
3) 180° rotation of LN plate around X-axis;
4) 180° rotation of LN plate around Y-axis.

It means that in the analyzed layered structure, the turnover of the LN plate required to switch between the "positive" and "negative" LN orientations can be replaced by rotation of a plate around any horizontal axis, either X or Y. Moreover, such turnover is similar to rotation of a substrate around the vertical Z-axis.

The results of 180° rotations of LN plate or quartz substrate around X-, Y-, or Z-axes are summarized in Table I. All rotated structures with acoustic wave behavior similar to the behavior in the initial LN/quartz structure are designated as "+," and inverted structures with alternative acoustic wave characteristics are designated as "−." All possible combinations of 180° rotations yield only two geometries of the layered structure. Due to the identical symmetry of LN and LT crystals, this analysis is also valid for LT/quartz structures with similar orientations. It is worth emphasizing that acoustic wave characteristics do not change with 180° rotations around the X-, Y-, or Z-axes in a regular single crystal substrate.

The numerical examples of asymmetry in LT/quartz structures presented in Section III-B include the discussion of the relation between this phenomenon and polarizations of acoustic waves propagating in different LT and quartz orientations. These structures combine a piezoelectric plate and a piezoelectric substrate, and the structures comprising a piezoelectric plate and a non-piezoelectric anisotropic substrate (LT/Si) are discussed in Section III-A. In addition, the effect of an isotropic layer introduced at the plate-substrate interface on asymmetry is also studied.

III. EXAMPLES OF ASYMMETRY IN LAYERED STRUCTURES

A. LT/Si and LT/SiO_2/Si Structures

Layered structures combining a thin LT or LN plate with a silicon (Si) substrate were investigated theoretically and experimentally by different research groups [1]–[6] as alternatives to single-crystal substrates. Leaky shear horizontally polarized (SH) waves generated in the regular LN and LT substrates and characterized by high electromechanical coupling factors transform into the non-leaky guided modes in thin LN or LT plates bonded to Si substrates. The transformation provided by faster bulk acoustic waves (BAWs) in Si enables the design of high-Q resonators.

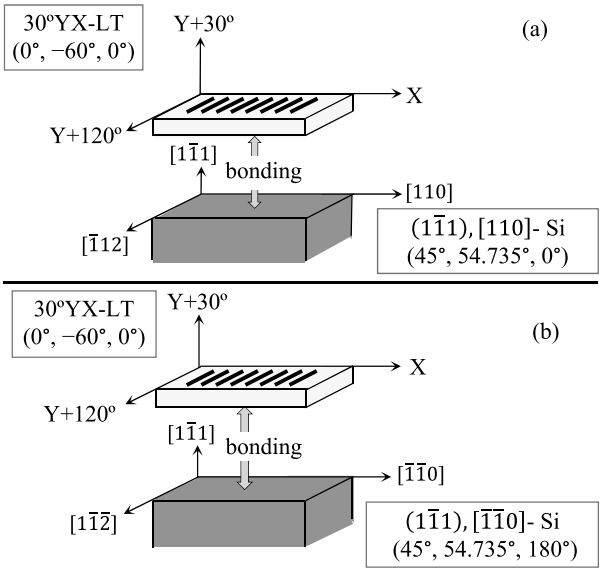

Fig. 3. Two analyzed LT/Si structures with 30° YX-LT plate bonded to (111),[110]-Si substrate and X-axis of LT parallel to (a) [110] or (b) [$\bar{1}\bar{1}$0] directions of Si.

In the most commonly used LT/Si structures, a thin plate of rotated YX cut of LT is bonded to ZX cut of Si substrate. Due to the alignment of the substrate surface and propagation direction with crystallographic axes of Si crystal, this substrate orientation ensures symmetric properties of a layered structure: the velocities of acoustic waves do not change with inversion of propagation direction in LT or Si, or with interchange of the top and bottom of the LT plate. However, asymmetry appears when Si substrate orientation changes. For example, if LT/Si interface is parallel to (1$\bar{1}$1) plane of Si, and the positive X-axis of LT is aligned either with [110] direction or with the opposite [$\bar{1}\bar{1}$0] direction of Si, then SH-SAW characteristics are different for these two structures.

The aforementioned structures are schematically shown in Fig. 3, where 30°YX cut of LT with Euler angles (0°, −60°, 0°) is combined with Si substrate defined by the angles (45°, 54.735°, 0°) [see Fig. 3(a)] or (45°, 54.735°, 180°) [see Fig. 3(b)]. The examples of resonator admittances obtained for these layered structures are plotted in Fig. 4. Three resonators have the same Al electrode thickness, $h_{\mathrm{Al}} = 0.05\lambda$, where $\lambda = 2p$ is acoustic wavelength and p is the periodicity of the electrode structure, but LT plate thickness h_{LT} varies between 0.05λ and 0.2λ. Asymmetry between the structures with initial (0°) and inverted (180°) propagation directions can be evaluated as the shifts of resonant and anti-resonant frequencies, $\Delta_R = [f_R(180°) - f_R(0°)]/f_R(0°)$ and $\Delta_A = [f_A(180°) - f_A(0°)]/f_A(0°)$. In the analyzed structures $\Delta_R > \Delta_A$, and maximum asymmetry occurs at $h_{\mathrm{LT}} = 0.1\lambda$.

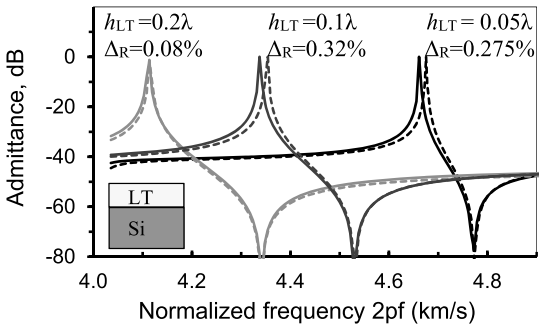

Fig. 4. Admittances Im(Y) of resonators using 30°YX-LT/(111),[110]-Si structures with initial (solid lines) and inverted (dashed lines) propagation directions in Si. Al electrode thickness is $h_{Al} = 0.05\lambda$ and LT thicknesses h_{LT} varies between 0.05λ and 0.2λ. Variation of resonant frequency Δ_R was estimated for each LT thickness.

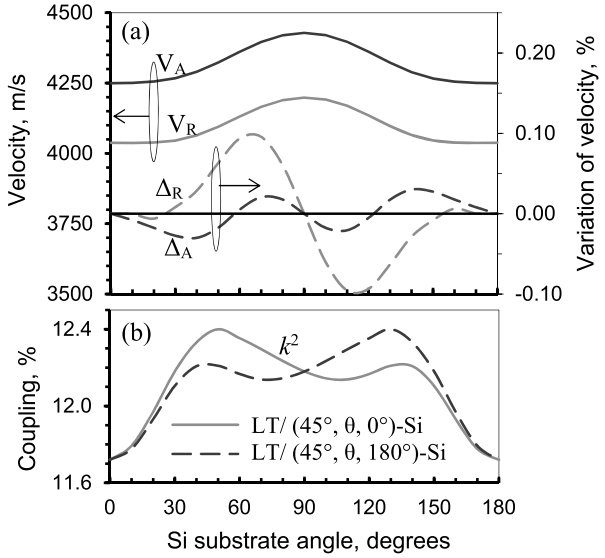

Fig. 5. SH-SAW characteristics in resonators based on 30° YX-LT/(45°, θ, 0°)-Si and 30° YX-LT/(45°, θ, 180°)-Si structures, as functions of Si substrate angle θ. (a) Velocities at resonance (V_R) and anti-resonance (V_A) and their variations with 180° rotation of Si substrate (Δ_R, Δ_A). (b) Electromechanical coupling k^2 in two structures. LT thickness is 0.2λ and Al electrode thickness is 0.05λ.

To estimate the influence of Si substrate orientation on asymmetry, admittance functions were calculated for resonators on 30°YX/Si with Si orientations defined by the angles (45°, θ, 0°) and (45°, θ, 180°), and the angle θ continuously changing between 0° and 180°. The resonant f_R and anti-resonant f_A frequencies were extracted for two opposite propagation directions in Si and further used for calculation of effective velocities V_R and V_A [see Fig. 5(a)] and electromechanical coupling coefficients k^2 [see Fig. 5(b)], as functions of the angle θ.

The shifts of resonant and anti-resonant frequencies, Δ_R and Δ_A, caused by inversion of the propagation direction in Si substrate and shown in Fig. 5(a), illustrate the dependence of asymmetry on Si substrate orientation. When $\theta = 0°$ or $\theta = 90°$, there is no asymmetry ($\Delta_R = \Delta_A = 0$). For other angles, both parameters become nonzero, and the analyzed structures demonstrate noticeable asymmetry. The resonant frequency is more sensitive to the inversion of Si

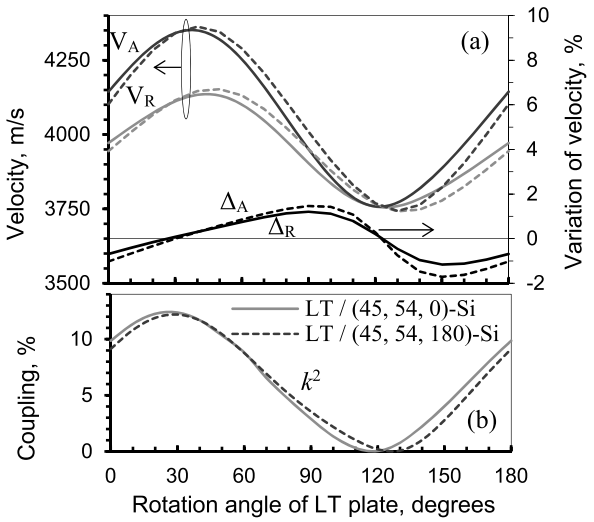

Fig. 6. SH-SAW characteristics in resonators on μ-rotated YX-LT bonded to (45°, 54°, 0°) and (45°, 54°, 180°)-Si substrates, as functions of angle μ. (a) Velocities at resonance (V_R) and anti-resonance (V_A) and their variations with 180°-rotation of Si substrate (Δ_R, Δ_A). (b) Eectromechanical coupling k^2 in two structures.

orientation, and Δ_R achieves maximum absolute values of ±0.1% when $\theta = 70°$ and $\theta = 110°$. Asymmetry shows an especially pronounced effect on the coupling coefficient k^2 [see Fig. 5(b)], which varies between 12.2% and 12.4% in some orientations. It means that LT and Si orientations should be verified carefully before bonding to ensure the required acoustic wave characteristics in the layered substrate.

According to the simulation results shown in Fig. 5, maximum asymmetry does not coincide with the maximum electromechanical coupling of the analyzed wave. It means that asymmetry cannot be explained only by the inversion of electric fields, and its nature is more complicated. The relationship between asymmetry and piezoelectric coupling was analyzed further for μ-rotated YX-LT plate, with μ varying between 0° and 180°, combined with (45°, 54°, 0°) or (45°, 54°, 180°)-Si substrate. Fig. 6 shows the calculated velocities, coupling k^2, and asymmetry parameters Δ_R and Δ_A of SH-SAWs propagating in these structures. Minimum asymmetry is expected in 30°YX and 120°YX cuts of LT. The coupling achieves maximum (12%) and minimum (zero) values, respectively, at these angles. Hence, there is no direct correlation between the piezoelectric coupling of the analyzed mode and asymmetry. Moreover, the contribution of the substrate anisotropy into asymmetry looks even more significant than the influence of electric fields generated in a piezoelectric plate.

Another significant factor that affects the asymmetry of a layered structure is the polarization of acoustic mode. Different asymmetry is observed for SH-SAW, Rayleigh SAW, and high-velocity leaky SAW propagating in the same layered structure. Fig. 7 shows admittance functions of resonators based on LT/Si structures, with ZX-cut [see Fig. 7(a)] or YX-cut [see Fig. 7(b)] of LT bonded to Si substrate defined by the Euler angles (45°, 54.735°, 0°) or (45°, 54.735°, 180°).

Two modes propagate in the analyzed frequency range: Rayleigh SAW and SH-SAW. The colored diagrams shown

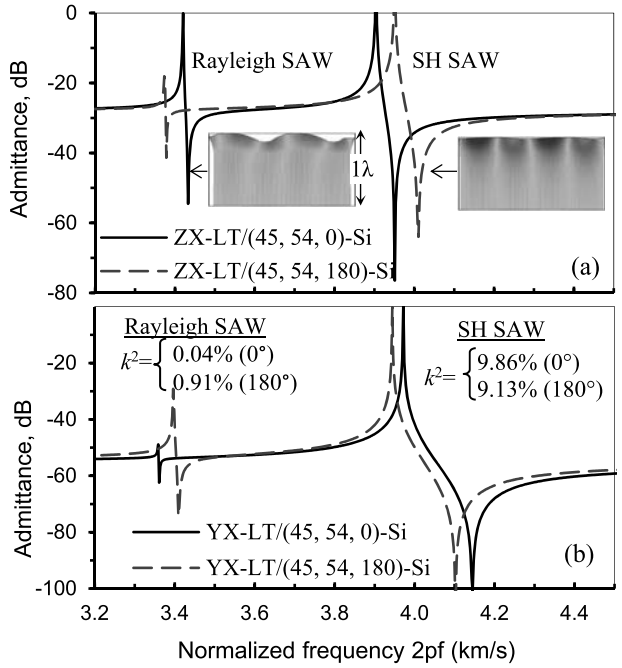

Fig. 7. Two examples of LT/Si structures characterized by large asymmetry: admittances of resonators using (a) *ZX*-LT/(45, 54.735, 0° ± 180°)-Si and (b) *YX*-LT/(45, 54.735, 0° ± 180°)-Si substrates. Inset: structure of two modes, with displacements in *XZ* plane shown as wave motions and color diagram referred to displacements along *Y*-axis (SH).

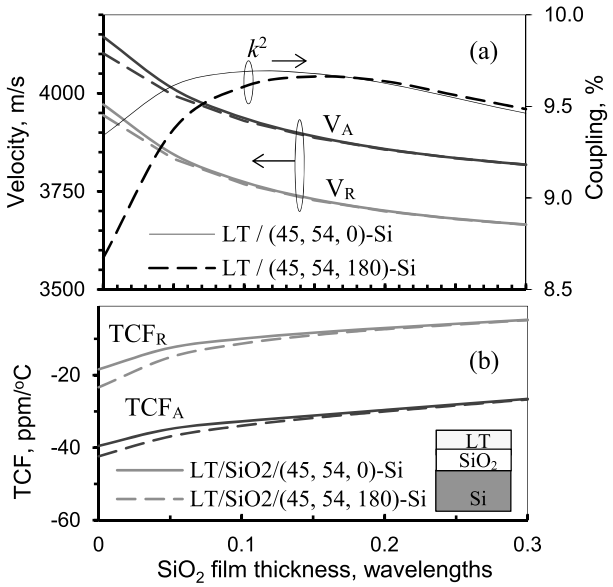

Fig. 8. SH-SAW characteristics at resonance (V_R) and anti-resonance (V_A) in resonators using *YX*-LT/SiO_2/(45°, 54.735°, 0° ± 180°)-Si structures, as functions of SiO_2 film thickness. (a) Velocities and coupling in two structures. (b) TCFs estimated at resonance (TCF_R) and anti-resonance (TCF_A).

in the inset of Fig. 7(a) illustrate the wave structures. The displacements caused by Rayleigh SAW are almost confined in the sagittal plane (*XZ*), while SH-SAW is polarized along *Y*-axis. In both structures shown in Fig. 7, asymmetry is markedly strong but different for two acoustic waves: one of the waves propagates slower in the inverted structure, while another wave propagates faster. In addition, the results of simulations demonstrate that 180° rotation of Si substrate can simultaneously enhance the main SH-SAW (its k^2 increases from 9.13% to 9.86%) and suppress the spurious Rayleigh SAW (k^2 decreases from 0.91% to 0.04%). Consequently, inversion of a substrate orientation can be a simple method of providing better resonator performance.

To improve the temperature characteristics of resonators using LT/Si structures, an intermediate isotropic SiO_2 layer is usually introduced between LT plate and Si substrate. The absolute values of TCFs estimated at resonant and anti-resonant frequencies decrease with SiO_2 film thickness and cross zero at certain film thicknesses. The presence of additional layer impacts asymmetry of the layered structure: it decreases and eventually vanishes with the localization of the wave energy in the isotropic SiO_2 layer instead of anisotropic Si substrate. This statement was verified by the simulations of resonator characteristics in *YX*-LT/SiO_2/(45°, 54.735°, 0° ± 180°)-Si structures with variable SiO_2 thickness (see Fig. 8).

In LT/Si structures without SiO_2 layer at the interface, SH-SAW velocities are different for opposite propagation directions (0° and 180°) in Si substrate, and the coupling k^2 varies between 9.3% and 8.7%. If SiO_2 intermediate layer is introduced and its thickness grows from zero to 0.3λ, TCF values at resonance (TCF_R) and anti-resonance (TCF_A) improve, respectively, from −40 to −26 and from −20 to −5 ppm/°, while asymmetry tends to 0. The analyzed LT and SiO_2 thicknesses are typical for SAW resonators with improved temperature characteristics based on LT/SiO_2/Si substrates. Therefore, in SAW devices with low TCF achieved due to thick SiO_2 interlayer, the effect of asymmetry can be ignored. Asymmetry also decreases if a polycrystalline Si "trap rich" layer is introduced between LT plate and Si substrate to eliminate the conductive after-bonding layer and improve the thermal stability of SAW resonators.

It should be mentioned that polarity inverted LT/Si structure can be obtained by 180° rotation of Si substrate around *Z*-axis or around *Y*-axis. All orientations providing two types of LT/Si structures can be described by Table I, if quartz orientations (0°, μ, 90°), (0°, 180° + μ, 90°), (180°, −μ, 90°), and (0°, μ, −90°) are replaced by Si orientations (45°, μ, 0°), (45°, 180° + μ, 0°), (45° ± 180°, −μ, 0°), and (45°, μ, 180°), respectively.

B. LT/Quartz: Asymmetry of SH SAW and LLSAW Modes

LT/quartz is another candidate of a layered substrate for SAW devices with improved performance. These structures were investigated theoretically and experimentally [17], [21]–[25] as potential substrates for high-*Q* resonators with improved temperature characteristics, due to high k^2 of SH-SAW combined with low propagation losses and improved TCF provided by selected quartz orientations.

The anisotropy of quartz and its specific temperature behavior enable the optimization of LT/quartz structures for SH-SAW resonators with low or even zero TCF. Moreover, high-frequency high-*Q* resonators employing high-velocity longitudinal leaky SAWs (LLSAWs) can be fabricated on LT/quartz and LN/quartz structures [4], [17]–[19], [21], [22]. However, strong anisotropy of quartz combined with nonzero

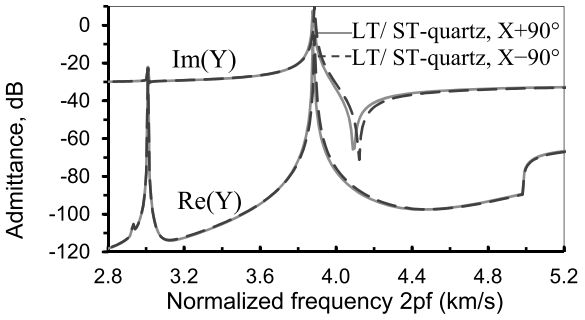

Fig. 9. Admittance of resonators based on LT/quartz structure: 30°LT/ST-quartz, with $X \pm 90°$ propagation directions. LT and Al electrode thicknesses are $h_{LT} = 0.15\lambda$, $h_{Al} = 0.08\lambda$.

piezoelectric constants assumes asymmetry of acoustic wave propagation in LT/quartz.

Fig. 9 shows the simulated admittances of resonators based on 30°LT/ST-quartz structure with $X + 90°$ and $X - 90°$ propagation directions in quartz. Two modes propagate in these structures: Rayleigh SAW with a velocity of about 3000 m/s and SH-SAW with an effective velocity at resonance $V_R \approx 3877$ m/s. Both values do not change noticeably with the 180° rotation of the substrate orientation. The anti-resonant frequency is more sensitive to the rotation, and the coupling k^2 of SH-SAW switches between 12.167% for $X + 90°$ and 13.13% for $X - 90°$ propagation directions. The spurious mode shows low coupling of about 0.03% for both directions. This example demonstrates that Rayleigh SAW and SH-SAW generally have different sensitivities to inversion of the substrate orientation. The difference between them follows from polarizations of the modes.

Though low TCF can be achieved for SH-SAWs propagating in some LT/quartz structures, resonant and anti-resonant frequencies demonstrate different temperature dependence, and the difference between TCF_R and TCF_A usually grows with the electromechanical coupling coefficient. However, some LT/quartz structures enable near-zero TCF values simultaneously at resonance and anti-resonance, $TCF_R \approx TCF_A \approx 0$, if the selected quartz orientation provides strong acoustic anisotropy [9], [24]. The optimal quartz orientations were previously determined as (70°–72°)-rotated Y-cuts with $X + 90°$ propagation direction [9]. LT plate orientation can vary in a wide angular range and is usually optimized to achieve high k^2 of SH-SAW.

Fig. 10 shows the calculated velocities, coupling k^2, and TCF as functions of LT cut angle when LT plate is combined with $71°Y$, $X \pm 90°$-quartz. The analyzed LT thickness is 0.15λ, and the Al electrode thickness is 0.08λ. The asymmetry effect observed as the difference between SH-SAW velocities in initial and inverted substrates (see Fig. 10) is nearly independent of the LT cut angle. Low TCF <10 ppm/°C can be obtained in (36°–60°)-YX cuts of LT, while k^2 varies in a wide range between 8% and 11% and achieves maximum in 20°YX LT. These simulations demonstrate that the influence of quartz substrate orientation on the asymmetry of LT/quartz structure is much stronger than the effect of LT plate orientation.

The last example illustrating asymmetry of wave characteristics in LT/quartz refers to the structure optimized for

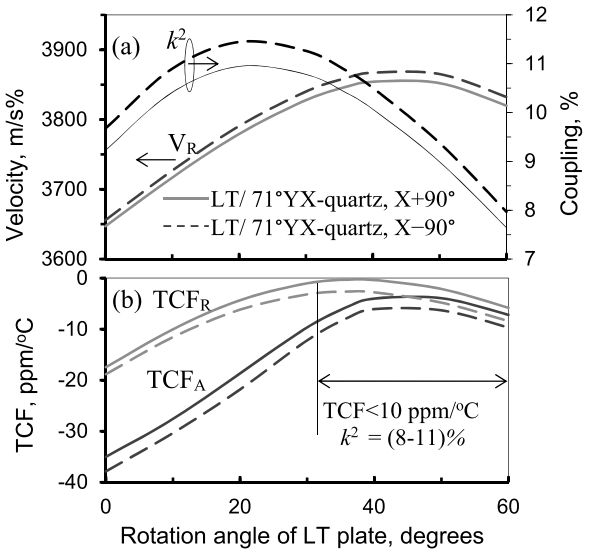

Fig. 10. SH-SAW characteristics as functions of LT orientation in LT/quartz structures with improved temperature characteristics. (a) Velocities and coupling in two structures. (b) TCFs estimated at resonance and anti-resonance. LT and Al thicknesses are $h_{LT} = 0.15\lambda$ and $h_{Al} = 0.08\lambda$.

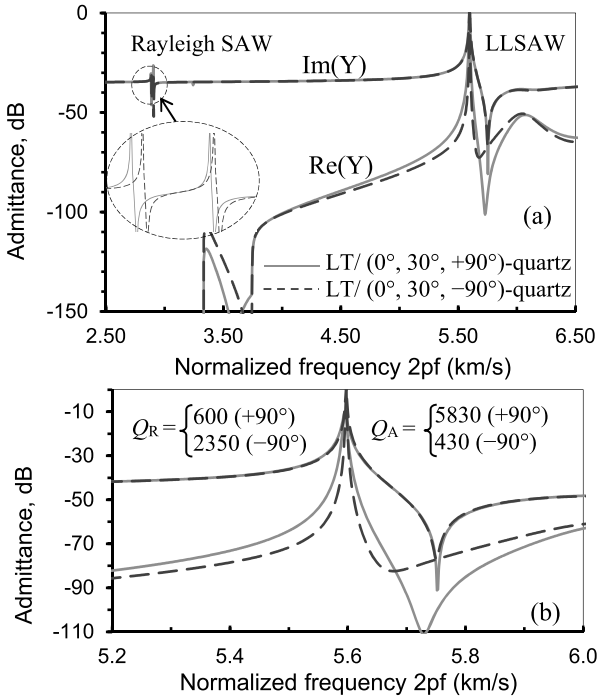

Fig. 11. Admittance of LLSAW resonator with Cu electrodes on (0°, 34°, 90°)-LT/(0°, 30°, ±90°)-quartz structure optimized for high Q factors. (a) Admittance in wide bandwidth with enlarged Rayleigh mode response. (b) Admittance referred to LLSAW mode and Q-factors estimated for two quartz orientations. LT and Cu thicknesses are $h_{LT} = 0.32\lambda$, $h_{Cu} = 0.05\lambda$. Duty factor is $a/p = 0.3$.

LLSAW resonators. The simulated admittance is plotted in Fig. 11. LLSAW resonator with Cu electrodes is based on (0°, 34°, 90°)-LT/(0°, 30°, 90°)-quartz structure. This layered structure was optimized previously to obtain high Q-factors of LLSAW resonators, and the found optimal LT and Cu thicknesses were 0.32λ and 0.05λ, respectively, with duty

factor $a/p = 0.3$ providing low LLSAW losses [17]. Fig. 11(a) shows resonator response simulated in a wide frequency range, with Rayleigh SAW and LLSAW modes generated at different frequencies. The increased fragment in the inset of Fig. 11(a) reveals two resonances referred to the lower and upper edges of the resonator stopband caused by Rayleigh SAW. This wave propagates with a velocity of 2700 m/s. Both resonances shift with the inversion of the quartz substrate.

The asymmetry of LLSAW [see Fig. 11(b)] can be observed as different behaviors of propagation losses in initial and inverted structures [Re(Y) in Fig. 11] and significant variation of Q-factors estimated at resonance (Q_R) and at anti-resonance (Q_A). When the propagation direction in quartz switches from $X + 90°$ to $X - 90°$, Q_R improves from 600 to 2350, while Q_A degrades from 5830 to 430.

IV. Conclusion

Asymmetry of acoustic wave propagation in layered structures, which is understood here as the dependence of wave characteristics on the inversion of propagation direction in one of the combined materials, is typical for layered structures including anisotropic and piezoelectric layers and requires careful control of crystal orientations before their bonding to ensure the required characteristics of SAW devices manufactured on the layered structure. This phenomenon arises from anisotropy of combined materials and occurs even when one of these materials is non-piezoelectric. The "polarity inverted" structure enabling alternative device performance for the same material layers can be obtained either by an interchange of top/bottom surfaces of a piezoelectric plate or by inversion of propagation direction in a substrate. Asymmetry depends on crystal orientations and polarization of acoustic waves and decreases with the introduction of an isotropic layer at the plate-substrate interface.

References

[1] M. Kadota and S. Tanaka, "Solidly mounted ladder filter using shear horizontal wave in $LiNbO_3$," in *Proc. IEEE Int. Ultrason. Symp. (IUS)*, Sep. 2016, pp. 1–4.

[2] T. Takai *et al.*, "High-performance SAW resonator on new multilayered substrate using $LiTaO_3$ crystal," *IEEE Trans. Ultrason., Ferroelectr., Freq. Control*, vol. 64, no. 9, pp. 1382–1389, Sep. 2017.

[3] T. Kimura *et al.*, "A high velocity and wideband SAW on a thin $LiNbO_3$ plate bonded on a Si substrate in the SHF range," in *Proc. IEEE Int. Ultrason. Symp. (IUS)*, Oct. 2019, pp. 1239–1248.

[4] M. Gomi, T. Kataoka, J. Hayashi, and S. Kakio, "High-coupling leaky surface acoustic waves on $LiNbO_3$ or $LiTaO_3$ thin plate bonded to high-velocity substrate," *Jpn. J. Appl. Phys.*, vol. 56, no. 7S1, 2017, Art. no. 07JD13.

[5] N. Naumenko, "Solidly mounted plate mode resonators based 42°-48°YX LT cuts: Loss mechanisms," in *Proc. IEEE Int. Ultrason. Symp. (IUS)*, Washington, DC, USA, Sep. 2017, pp. 1–4.

[6] N. F. Naumenko, "Multilayered structures using thin plates of $LiTaO_3$ for acoustic wave resonators with high quality factor," *Ultrasonics*, vol. 88, pp. 115–122, Aug. 2018.

[7] M. Kadota and S. Tanaka, "Wideband acoustic wave resonators composed of hetero acoustic layer structure," *Jpn. J. Appl. Phys.*, vol. 57, no. 7S1, Jul. 2018, Art. no. 07LD12.

[8] M. Kadota, Y. Ishii, and S. Tanaka, "Surface acoustic wave resonators with hetero acoustic layer (HAL) structure using lithium tantalate and quartz," *IEEE Trans. Ultrason., Ferroelectr., Freq. Control*, vol. 68, no. 5, pp. 1955–1964, May 2021.

[9] N. F. Naumenko, "Temperature behavior of SAW resonators based on $LiNbO_3$/quartz and $LiTaO_3$/quartz substrates," *IEEE Trans. Ultrason., Ferroelectr., Freq. Control*, vol. 68, no. 11, pp. 3430–3437, Nov. 2021, doi: 10.1109/TUFFC.2021.3089481.

[10] J. W. Strutt, "Some general theorems relating to vibrations," *Proc. London Math. Soc.*, vol. 4, no. 1, pp. 357–368, Nov. 1873.

[11] N. Naumenko, "Asymmetry of acoustic wave propagation in layered structures," in *Proc. IEEE Int. Ultrason. Symp. (IUS)*, Sep. 2021, pp. 1–4.

[12] A. N. Stroh, "Steady state problems in anisotropic elasticity," *J. Math. Phys.*, vol. 41, nos. 1–4, pp. 77–103, Apr. 1962.

[13] E. L. Adler, "Matrix methods applied to acoustic waves in multilayers," *IEEE Trans. Ultrason., Ferroelectr., Freq. Control*, vol. 37, no. 6, pp. 485–490, Nov. 1990.

[14] K. A. Ingebrigtsen and A. Tonning, "Elastic surface waves in crystals," *Phys. Rev.*, vol. 184, no. 3, pp. 942–951, Aug. 1969.

[15] K. A. Ingebrigtsen and A. Tonning, "Excitation of elastic waves in crystals," *IEEE Trans. Microw. Theory Techn.*, vol. MTT-17, no. 11, pp. 827–835, Nov. 1969.

[16] N. F. Naumenko, "Advanced numerical technique for analysis of surface and bulk acoustic waves in resonators using periodic metal gratings," *J. Appl. Phys.*, vol. 116, no. 10, Sep. 2014, Art. no. 104503.

[17] N. F. Naumenko, "High-velocity non-attenuated acoustic waves in $LiTaO_3$/quartz layered substrates for high frequency resonators," *Ultrasonics*, vol. 95, pp. 1–5, May 2019.

[18] N. Naumenko, "$LiNbO_3$ plate bonded to quartz as a substrate for high frequency wideband SAW devices," in *Proc. IEEE Int. Ultrason. Symp. (IUS)*, Oct. 2019, pp. 1227–1230.

[19] N. F. Naumenko, "Optimization of $LiNbO_3$/quartz substrate for high frequency wideband SAW devices using longitudinal leaky waves," *IEEE Trans. Ultrason., Ferroelectr., Freq. Control*, vol. 67, no. 7, pp. 1485–1491, Jul. 2020.

[20] N. F. Naumenko, "Advanced substrate material for SAW devices combining $LiNbO_3$ and langasite," *IEEE Trans. Ultrason., Ferroelectr., Freq. Control*, vol. 67, no. 9, pp. 1909–1915, Sep. 2020.

[21] J. Hayashi *et al.*, "High coupling and highly stable leaky surface acoustic waves on $LiTaO_3$ thin plate bonded to quartz substrate," *Jpn. J. Appl. Phys.*, vol. 57, no. 7S1, Jun. 2018, Art. no. 07LD21.

[22] J. Hayashi *et al.*, "Longitudinal leaky surface acoustic wave with low attenuation on $LiTaO_3$ or $LiNbO_3$ thin plate bonded to quartz substrate," *Jpn. J. Appl. Phys.*, vol. 58, no. SG, Jul. 2019, Art. no. SGGC12.

[23] N. Naumenko, "Suppression of propagation losses in TC SAW resonators using thin plates of $LiTaO_3$ bonded to quartz substrates," in *Proc. IEEE Int. Ultrason. Symp. (IUS)*, Oct. 2018, pp. 1–9.

[24] S. Inoue and M. Solal, "Spurious free SAW resonators on layered substrate with ultra-high Q, high coupling and small TCF," in *Proc. IEEE Int. Ultrason. Symp. (IUS)*, Oct. 2018, pp. 1–9.

[25] S. Inoue and M. Solal, "Layered SAW resonators with near-zero TCF at both resonance and anti-resonance," in *Proc. IEEE Int. Ultrason. Symp. (IUS)*, Oct. 2019, pp. 2079–2082.

Natalya F. Naumenko (Member, IEEE) received the M.Sc. and Ph.D. degrees in physics of dielectrics and semiconductors from Moscow Technological University (MISIS), Moscow, Russia, in 1979 and 1984, respectively.

From 1995 to 2011, she was a Consultant in materials for surface acoustic wave (SAW) devices for the companies SAWTEK and TriQuint Semiconductors, Apopka, FL, USA. Since 2011, she has been a Consultant and performed research project for different SAW companies: TDK-EPCOS, Munich, Germany, CTR, Villach, Austria, and HUAWEI, Shanghai, China. She is currently with the Acoustooptical Research Center, National University of Science and Technology MISIS, Moscow, and with the Research Department, Moscow Technical University of Communications and Informatics, Moscow. She has authored 16 issued U.S. patents and more than 100 publications in SAW material research. Her current research interests include different aspects of acoustic wave propagation in crystals and multilayered structures, and development of improved simulation tools for design of SAW and bulk acoustic wave (BAW) devices, such as resonator SAW filters, delay lines, and wireless SAW sensors.

Dr. Naumenko has been a member of the Technical Program Committee of the IEEE Ultrasonic Symposium since 2011.